

1-1-2022

Geochemical and petrographic approach for the origin of the limestone blocks of the walls of the Great Temple of Hattusha, Çorum (N-Turkey)

İSMAİL ÖMER YILMAZ

ANDREAS SCHACHNER

İBRAHİM TONGUÇ UYSAL

EZGİ ÜNAL İMER

Follow this and additional works at: <https://journals.tubitak.gov.tr/earth>



Part of the [Earth Sciences Commons](#)

Recommended Citation

YILMAZ, İSMAİL ÖMER; SCHACHNER, ANDREAS; UYSAL, İBRAHİM TONGUÇ; and İMER, EZGİ ÜNAL (2022) "Geochemical and petrographic approach for the origin of the limestone blocks of the walls of the Great Temple of Hattusha, Çorum (N-Turkey)," *Turkish Journal of Earth Sciences*: Vol. 31: No. 3, Article 10. <https://doi.org/10.55730/1300-0985.1774>

Available at: <https://journals.tubitak.gov.tr/earth/vol31/iss3/10>

This Article is brought to you for free and open access by TÜBİTAK Academic Journals. It has been accepted for inclusion in Turkish Journal of Earth Sciences by an authorized editor of TÜBİTAK Academic Journals. For more information, please contact academic.publications@tubitak.gov.tr.

Geochemical and petrographic approach for the origin of the limestone blocks of the walls of the Great Temple of Hattusha, Çorum (N-Turkey)

İsmail Ömer YILMAZ^{1*}, Andreas SCHACHNER², İ. Tonguç UYSAL³, Ezgi ÜNAL-İMER¹

¹Department of Geological Engineering, Middle East Technical University, Ankara, Turkey

²Department of Geological Engineering, German Archaeological Institute, İstanbul, Turkey

³Department of Geology Engineering, Faculty of Engineering, İstanbul-Cerrahpaşa University, İstanbul, Turkey

Received: 04.03.2021 • Accepted/Published Online: 09.05.2022 • Final Version: 18.05.2022

Abstract: The socle stones of the Great Temple in the Lower City of the Hittite capital city, Hattusha (Çorum Province) have been studied for the first time by petrographic and geochemical analysis (Sr isotope, stable isotope, and trace element geochemistry). Study objectives were to determine the carbonate facies of the stone samples used in the Great Temple and investigate their possible sources. Petrographic analysis of 10 limestone samples presents five clusters of different microfacies. Stable isotope ($\delta^{13}\text{C}$ and $\delta^{18}\text{O}$) analysis displayed the presence of 5 groups in parallel with petrographic analysis. Trace element analysis of the same groups displayed considerable difference among the stone samples and $^{87}\text{Sr}/^{86}\text{Sr}$ isotope ratios change between 0.70697 and 0.706867. Based on the results, it can be stated that the building using stones are from probably five different sources. This is of great importance to better understand the construction process and the acquisition of the building materials.

Key words: Hattusha, Great Temple, building stone, sedimentary geochemistry, archaeometric study, N-Turkey

1. Introduction

Due to its availability, the stone is one of the most ancient and most common building materials used by humans (Siegesmund and Török, 2014). Studies in archeological geology cover different disciplines and various types of applications. Analysis of mosaics, sculptures, and ceramics by sedimentology, petrography, mineralogy and/or geochemistry are common studies to determine especially the provenance of archeological materials (Flügel, 2010a, 2010b, 2010c; Price and Button, 2012; Hunt, 2013 among many others).

Apart from archaeometric studies focusing on the origin of marble used for construction of buildings, only a few studies deal with the provenance of stone building material from archeological sites of the Bronze and Classical Ages in Turkey. This is mainly due to the fact that in most cases very small pieces of broken stone were used for the construction of the walls so a satisfying sample strategy is impossible to be applied. The analysis of large quantities of such small stones necessary to achieve a statistically reliable result would need a technical, laboratory, and funding effort that cannot be carried out. On the other hand, the analysis of large, carefully worked stones, which were usually used for monumental public

buildings, allows conclusions to be drawn not only about the sources of the stones, but also about the division of labor during their extraction and processing. Among others, research at Boğazköy-Hattusha (Akar et al., 2009; Flügel, 2010b; Akcar et al., 2014; Yilmaz et al., 2014), the capital city of the Hittite Empire in the Late Bronze Age (Schachner, 2011), and Sagalassos (Braekmans et al., 2016) may be mentioned as examples of attempts to pinpoint the sources of the stones used for the construction of unique buildings.

In Hattusha, since 1986 a UNESCO world-heritage (<https://whc.unesco.org/en/list/377>) site located in Çorum Province, northeastern part of Central Anatolia, a first exemplary comparative research on the worked building stones from Yenicekale has already shown potential of this approach. Although some material might have been taken from the underlying host rock itself when it was leveled, the majority of the building stones were brought to the building site from different sources in, as well as outside, the city. One quarry approximately 2.5 km southeast of the city could be identified with high probability (Akar et al., 2009; Yilmaz et al., 2014). The promising results of this pilot study proving the method of petrographic comparison to be a fruitful approach was the starting point

* Correspondence: iyilmaz@metu.edu.tr

for a more comprehensive work focusing on the building stones of the Great Temple in the Lower City of the Hittite capital city.

The site of present-day Boğazkale (until 1982 Boğazköy; located roughly 180 km east of Ankara) served as the capital city of the Hittite Empire for more than 400 years roughly between 1650 and 1180 BCE (Schachner 2011; 2019; for the Hittite Empire and its culture in general cf. the articles in Doğan-Alparslan and Alparslan 2013). The founding of the first Anatolian empire marks a deep change in the political and societal history of Asia Minor and is best represented by the monumental architecture resembling its state institutions (Schachner in press).

Among the many official Hittite edifices, the Great Temple in Hattusha stands out not only for its extraordinary preservation, but also for its technical and structural execution which is unique for its time and characterizes it as one of the key monuments of the Hittite era (Schachner 2020). In contrast to any other major Hittite construction, the socles of the walls are made of large neatly worked limestone blocks. The persevered part of the building comprises 454 blocks of varying sizes. One of the largest in the southeastern corner of the building measures approximately $5 \times 1, 7 \times 1.5$ m. The size and unchanged position of these blocks make the effort worth to further study their petrology and mineralogy.

The Late Bronze Age city is divided into several topographically defined functional units of which the Lower City belongs to the oldest part of the urban structure (Schachner, 2011; 2019). The so-called Great Temple (or Temple 1) represents one of the largest buildings of its period and dominates this part of the city being located at $40^{\circ}01'11.92''$ N and $34^{\circ}36'55.62''$ E (Schachner, 2011; Schachner, 2020 with further readings). The building was probably erected already in the old-Hittite period (c. 1650–1550/30 BC) and functioned as the most important sanctuary of the Hittite empire. Within the building, up to 7 groups of rooms are to be identified as sacred. Two chambers organized parallel side-by-side on the northern side of the sanctuary are most probably to be identified as the holy rooms of the two most important gods of the Hittite pantheon: the weather-god of Hatti and the sun-goddess of Arinna (Schachner 2020). In contrast to the majority of the building for which limestone was used, these two most important rooms and a few adjacent spaces were erected using gabbro (Figure 1). Our study focuses on the limestone parts of the edifice.

These very large and carefully worked limestone blocks can reach dimensions of up to $5 \times 1.70 \times 1.8$ – 2 m ($= 15$ – 18 m³). The distribution of the collected samples and the groups of their facies shown in different colors can be seen on the map of the Great Temple (Figure 1).

2. Geographic location and geological setting

Geographically, the study area lies in the Lower City of the Hittite capital Hattusha, which is located immediately south east of the modern district township of Boğazkale, which is part of Çorum Province in the northeast of Central Anatolia (Figure 2).

Geologically, the Hattusha lies on the İzmir-Ankara-Erzincan Suture Zone and was founded on the Ankara Mélange that is composed of marine sediments and mafic and ultramafic rocks of oceanic crust. Rock formations cropping out in its vicinity (Figure 3) are a sedimentary mélangé which is composed of blocks of Jurassic-Cretaceous limestones, volcanic rocks (Andesite Basalt or others) and volcanoclastic/siliciclastic matrix and the Ophiolitic Mélange cf. in general Kazancı et al. (2008). An Eocene flysch sequence composed of an alternation of turbiditic sandstones and mudstones crops outside the ancient city. Jurassic-Cretaceous limestones blocks are composed of pelagic and shallow water carbonates including reefal and neritic facies (Akçar et al., 2009 and Yılmaz et al., 2014). Ophiolitic mélangé is composed of igneous and volcanic blocks, pillow basalts, reddish radiolarian cherts, and serpentinized blocks and matrix. Limestone blocks are embedded in volcanic/volcanoclastic and siliciclastic matrix. Ophiolitic mélangé and sedimentary mélangé trust over each other and Eocene flysch trust over both of them (Şenel et al., 2002). The Great Temple within the city is located on the sedimentary mélangé and constructed mainly on limestone blocks.

3. Methodology

During fieldwork, very small samples from the still in situ building blocks of the Great Temple were derived from inside of the fractures. Collected samples do not disturb the original features of the blocks which are around 1 m in thickness. Samples were packed, sealed, registered, and sent with permission by the national museum at Çorum. Samples were examined for sedimentary and petrographic properties by thin sections under a Nikon research microscope in the sedimentology laboratory of the Department of Geological Engineering, Middle East Technical University, and microfacies of each sample were determined by visual estimation.

Samples collected for geochemical analysis were selected from pieces that are well preserved, unaltered and free of veins. Powdered samples are obtained by micromill drilling. Carbonate $\delta^{13}\text{C}$ and $\delta^{18}\text{O}$ isotope ratio analyses were conducted in the Stable Isotope Geochemistry Laboratory (SIGL) at University of Queensland (UQ). Pure calcite samples (3–4 mg, powdered) were analyzed using an Isoprime Dual Inlet Isotope Ratio Mass Spectrometer (DI-IRMS) with a Multiprep attached. Samples were reacted with orthophosphoric acid at 90 °C for 1000 s.

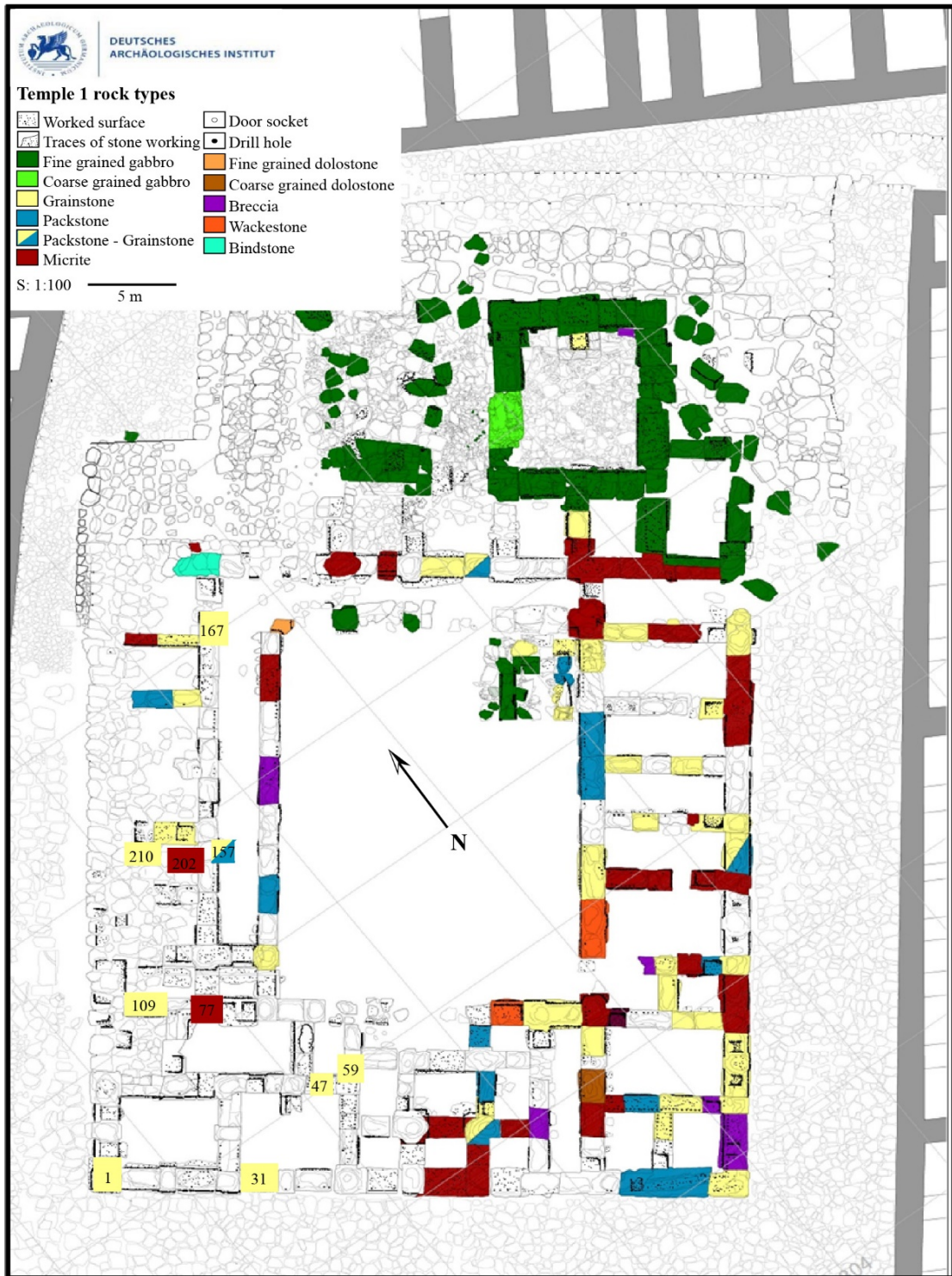


Figure 1. Studied samples and the distribution of their facies type groups in the Great Temple of Hattusha.

Stable isotope analytical results are reported in per mil (‰) relative to VPDB for oxygen and carbon with analytical uncertainties better than $\pm 0.2\text{‰}$ (2 σ) for both $\delta^{13}\text{C}$ and $\delta^{18}\text{O}$ (Table 1). The measurements were calibrated against NBS-

19 and NBS-18 international standards and analyzed as unknowns in addition to an internal laboratory standard.

A total of 10 carbonate samples were analyzed for their trace element concentrations using Thermo X-series II



Figure 2. Location map of the study area (Hattusha).

ICP-MS equipped with an ESI FC4 autosampler, UQ. A procedure modified after Eggins et al. (1997) and Kamber et al. (2003) was followed for measurement. About 50 mg of samples were digested in 2 mL of 15.8 N double distilled HNO_3 solution. A small aliquot of each sample was transferred into tubes and spiked with the internal standards (^7Li , ^{103}Rh , ^{115}In , ^{187}Re , ^{209}Bi , and ^{235}U). These solutions were further diluted using 2% HNO_3 for a dilution of ~4000 times in the final solution. Obtained raw signals were corrected for the background/blank signals, for the internal and external drift, and for oxide and double charge interference. Element concentrations (reported in ppb; Table 2) were calibrated against the elemental concentration of the USGS W-2 diabase rock standard.

Sr isotopic ratios of 10 samples reported in Table 2 were measured on a VG sector-54 thermal ionization mass spectrometer (TIMS) in the RIF Laboratory (UQ). They were corrected for mass discrimination using $^{86}\text{Sr}/^{88}\text{Sr}$ ratio = 0.1194. National Institute of Standards and Testing (NIST) SRM-987 Sr-isotope standard was used to monitor instrument drift and bias. Repeated analyses (no data outlier exclusion) of SRM-987 during January–May 2012 yielded an average $^{87}\text{Sr}/^{86}\text{Sr}$ value of 0.710222 ± 20 (2σ), which was used to calibrate against the laboratory's previous long-term mean, 0.710249 ± 28 (2σ) for all samples.

Sedimentary petrographic analyses have been conducted in the sedimentology laboratory of the Department of Geological Engineering, Middle East

Technical University, Ankara, Turkey. Petrographic and microfacies analysis of samples are carried out by using visual estimation for rock components, matrix, and cement on the thin sections with an Olympus CX31 polarizing microscope, and principles of microfacies analysis of Flügel (2010) have been followed.

4.1. Petrographic analysis

Petrographic determinations display that all samples are pure limestones, there are no traces of any clay or siliciclastic contributions. They can be listed as biomicrite, pelsparite, biopelsparite, intraclastic pelsparite, oolitic pelsparite, oosparite, intrasparite, and ooidal intrasparite. Although microfacies are generally different from each other, some samples are close in terms of composition.

Microfacies of 10 samples have been determined and it was recognized that clusters in stable isotope values also display differences in microscopic properties. Cluster 1 displays microfacies as: pelsparite mudstone contact, pelsparite, biopelsparite/biomicrite, biopelsparite/biomicrite (Figures 4a, 4b, 4e, 4h, 5e). Cluster 2 presents as intraclastic biopelsparite/pelsparite microfacies (Figures 4g, 4j, 5b–5d). Cluster 3 displays microfacies of oolitic pelsparite/intrasparite/oosparite and intrasparite/biosparite (Figure 4d). Cluster 4 presents as ooidal intrasparite microfacies (Figure 4f), and Cluster 5 presents as microfacies of intraclastic pelsparite (Figures 4c, 4i, 5f). Although there are some overlapping microfacies among the clusters, common microfacies belonging to each cluster display apparent differences.

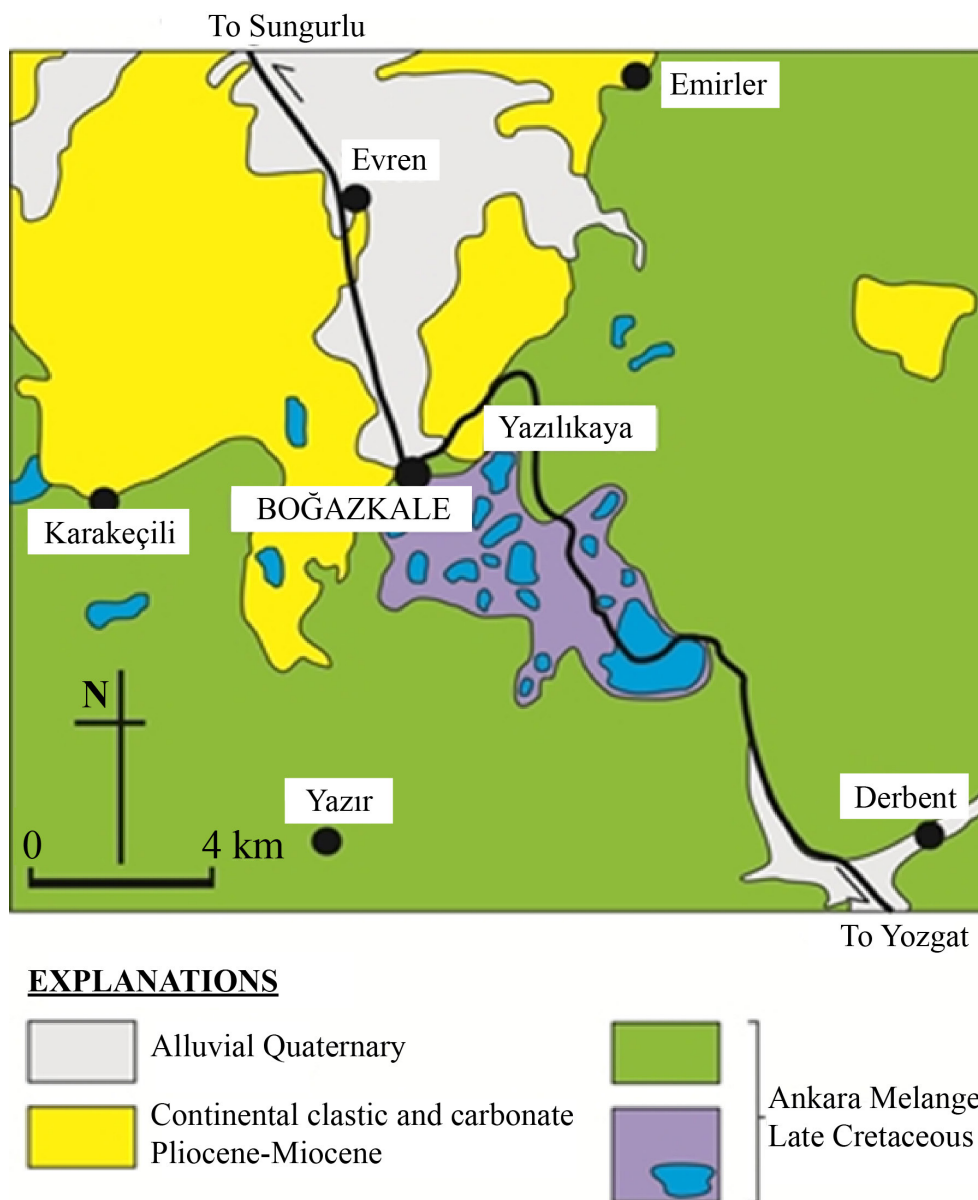


Figure 3. Geological map of the studied region (Şenel et al., 2002; MTA, 1/500 000 scaled maps).

Samples analyzed are collected from thick-very thick bedded limestone blocks along the wall of the main temple (Figure 5a) and the petrographic analyses and facies and textures recognized on the field such as breccia, dissolution vugs, infillings, fossil bioclasts, indicated that possible depositional environments are “inner platform” (Figures 4a–4f, 4h), “reef” (Figure 4i) and “slope” (Figures 4j and 4g) (Flügel 2010). This indicates that samples are originated from different sources and environments.

4.2. Geochemical analysis

Stable isotope analyses indicated 5 groups according to their $\delta^{13}\text{C}$ and $\delta^{18}\text{O}$ isotope values (Table 1; Figure 6). Group 1 displays an average of $\delta^{13}\text{C}$ values as 3.467943 per

mil and $\delta^{18}\text{O}$ values as -0.10841 per mil (VPDB). Group 2 presents $\delta^{18}\text{O}$ and $\delta^{13}\text{C}$ as -0.46918 per mil, 3.610557 per mil (VPDB), respectively. Group 3 displays average values of $\delta^{18}\text{O}$ and $\delta^{13}\text{C}$ as -0.76762 , 3.756123 per mil, respectively. Similar to group 2, group 4 presents $\delta^{18}\text{O}$ and $\delta^{13}\text{C}$ values as -1.17223 , 2.940174 per mil, respectively. Group 5 displays average values of $\delta^{18}\text{O}$ and $\delta^{13}\text{C}$ as -2.24651 , 3.298059 , respectively. These groups can easily be seen on $\delta^{13}\text{C}$ vs $\delta^{18}\text{O}$ graph as separated from each other (Figure 6).

Trace element analysis of the same clusters of the stable isotope analyses display considerable differences between them. Based on the REE+Y element diagram normalized

Table 1. Stable (O and C) isotope ratios of selected stone samples from Hattusha.

Sample number	$\delta^{18}\text{O}$ (‰, V-PDB)	$\delta^{13}\text{C}$ (‰, V-PDB)
1	-0.081	3.373
31	-0.087	3.458
47	-2.406	3.055
59	-0.740	3.852
77	-0.166	3.462
109	-1.172	2.940
157	-0.795	3.660
167	-0.469	3.611
202	-0.100	3.579
210	-2.087	3.541

Table 2. List of element data (ppb) and Sr isotope values of the studied carbonate samples.

Sample number	1	31	47	59	77	109	157	167	202	210
La	0.075	0.057	3.414	2.125	2.902	5.701	2.691	2.624	1.778	1.921
Ce	0.009	0.007	0.928	0.447	0.692	1.637	0.706	0.561	0.567	0.438
Pr	0.039	0.026	0.415	0.229	0.313	0.717	0.312	0.307	0.223	0.240
Nd	0.043	0.030	1.684	0.924	1.264	2.904	1.268	1.207	0.908	0.966
Sm	0.044	0.029	0.293	0.155	0.212	0.520	0.216	0.206	0.159	0.172
Eu	0.054	0.036	0.071	0.039	0.051	0.125	0.054	0.049	0.041	0.000
Gd	0.074	0.047	0.393	0.228	0.292	0.701	0.318	0.275	0.224	0.228
Tb	0.067	0.041	0.056	0.033	0.042	0.099	0.045	0.039	0.032	0.033
Dy	0.078	0.046	0.359	0.218	0.278	0.627	0.282	0.260	0.209	0.217
Y	0.204	0.117	4.740	3.515	4.174	7.866	4.380	3.847	3.105	2.794
Ho	0.087	0.052	0.088	0.057	0.070	0.150	0.071	0.066	0.052	0.051
Er	0.091	0.051	0.249	0.162	0.201	0.415	0.201	0.193	0.152	0.148
Tm	0.090	0.051	0.034	0.022	0.027	0.054	0.027	0.027	0.021	0.020
Yb	0.077	0.040	0.196	0.127	0.157	0.316	0.153	0.158	0.126	0.119
Lu	0.079	0.039	0.028	0.019	0.023	0.045	0.022	0.024	0.018	0.018
Y/Ho	2.349	2.248	53.704	61.771	59.905	52.444	61.694	58.671	59.167	54.459
$^{87/86}\text{Sr}$	0.70688	0.70693	0.70691	0.70687	0.70692	0.70697	0.70690	0.70694	0.70687	0.70690

to Post-Archaean Australian Shale (PAAS) (Taylor and McLennan, 1985) (Figure 7), the samples show two groups: one with negative Ce and positive Ho anomalies (samples 77, 202, 59, 157, 210, 47, 109, and 167), and the other with negative Ce and negative Ho anomalies (samples 1 and 31). These anomalies suggest conditions similar to near-surface (and low temperature) carbonate and/or chemical sedimentary rocks derived from seawater. The first group does not display remarkable increases in REE values, but

the second group does show an increase in the values from LREE to HREE, suggesting enrichment in the HREE in this group of carbonates. The La/Lu and Y/Ho ratios of the samples are different from each other, averaging at around 92 and 47, respectively (Table 2) (Taylor and McLennan, 1985).

$^{87}\text{Sr}/^{86}\text{Sr}$ isotope ratios of the carbonate samples vary between 0.70697 and 0.706867 and display a negative correlation with the $\delta^{13}\text{C}$ values (Figure 8). However,

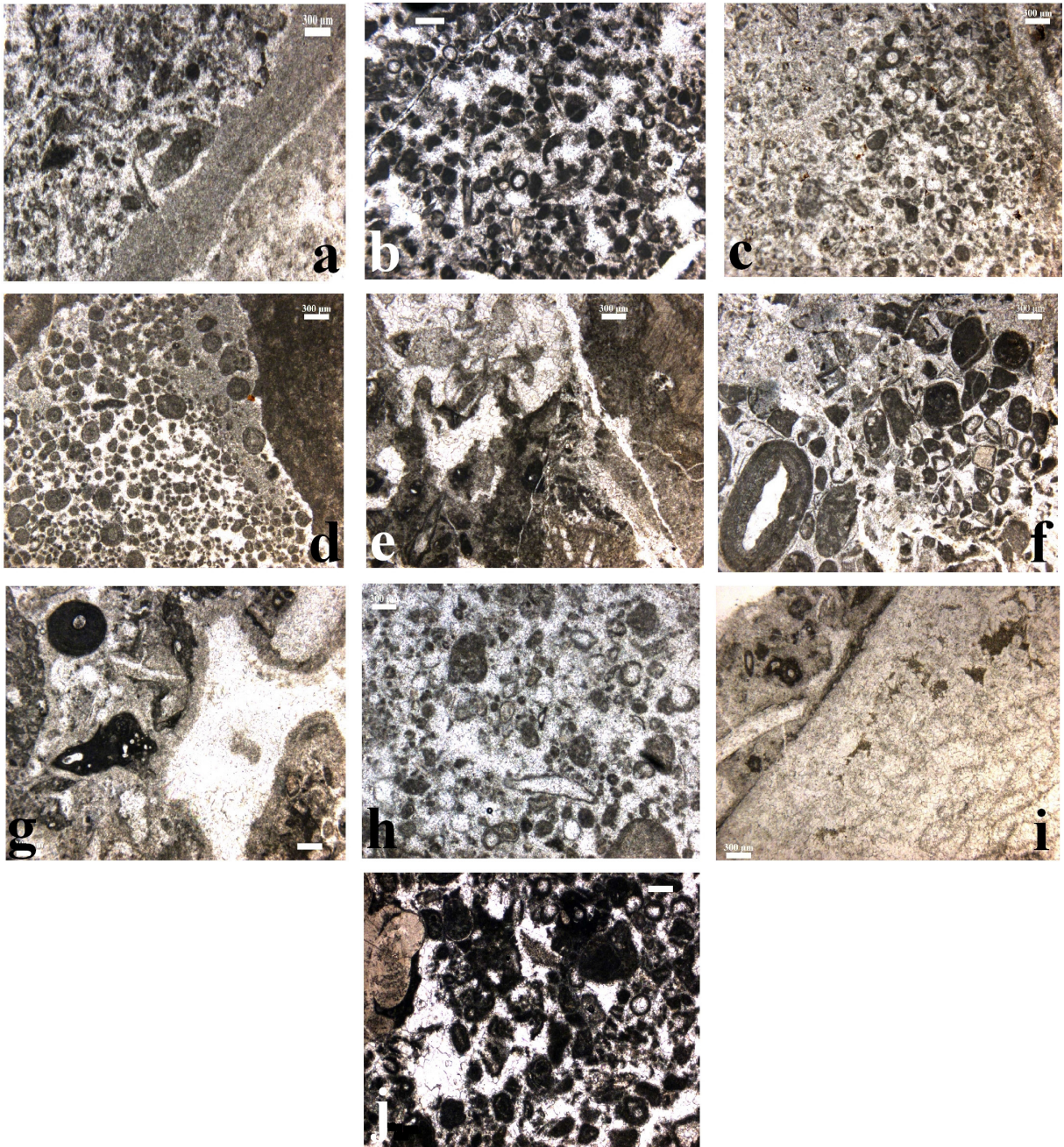


Figure 4. Photomicrographs of analyzed samples, a) biopelsparite/pelloidal grainstone with micrite contact (sample no: 1), b) pelsparite/pelloidal grainstone (sample no: 2), c) Biopelsparite/Intrasparite/pelloidalintraclastic grainstone (sample no: 31), d) oosparite/ooidalpelloidal grainstone (sample no: 59), e) biomicrite with calcite patches/lime mudstone with sparry calcite fillings (sample no: 77), f) oosparite/ooidal intraclastic grainstone (sample no: 109), g) Intrasparite/Intraclastic rudstone (sample no: 157), h) biopelsparite/biolcastic pelloidal grainstone (sample no: 167), i) biopelmicrite with coral fragments/lime mudstone (sample no: 202), j) biopelsparite/biolcastic pelloidal grainstone (sample no: 210).

$^{87}\text{Sr}/^{86}\text{Sr}$ isotopic values do not have a distinct relation with $\delta^{18}\text{O}$ values. Higher $\delta^{13}\text{C}$ values and lower $^{87}\text{Sr}/^{86}\text{Sr}$ isotope ratios indicate pure Jurassic carbonate values, although some samples show Cretaceous values according to the Sr isotope range only.

5. Discussion

This study has been carried out by the consent of Ministry of Culture and Tourism, Museum Directory and German Archeology Institute. Selection of samples and number of



Figure 5. Field photographs of the wall blocks of the Great temple, a) general view of the thick-very thick bedded limestone blocks along the wall (looking towards west), b) limestone block with bioclastic facies (sample 210), c) close up view of b, d) limestone block with breccia facies including intrclasts (sample 157), e) limestone block with intralcast and fossils (sample 167), f) Limestone block with pelloidal, intraclastic facies (sample 31).

samples were limited. Outside of the archeological side, number of visited quarries is 3, 2 of them were sampled, but number of visited outcrops is more than 50. Samples were already assigned in Yilmaz et al. (2019) and Akcar et al. (2009). There seems to be a relationship between use of

stones and analyzed samples in the temple, but to reach a definite conclusion, more samples must be analyzed.

Detailed future studies of the surrounding limestone sources will deliver more detailed explanations of the provenance of the monumental building stones from the

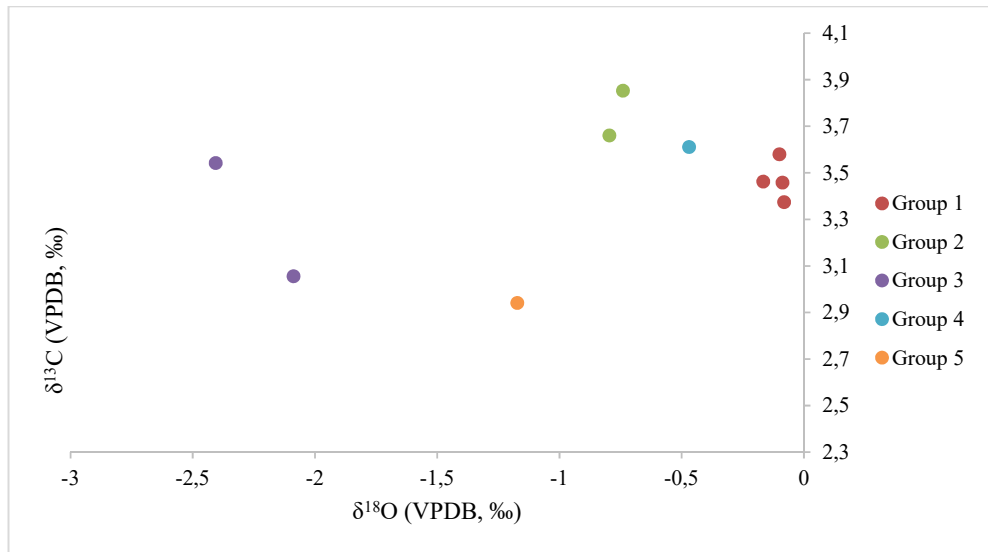


Figure 6. Stable (O and C) isotope results of the selected carbonate samples.

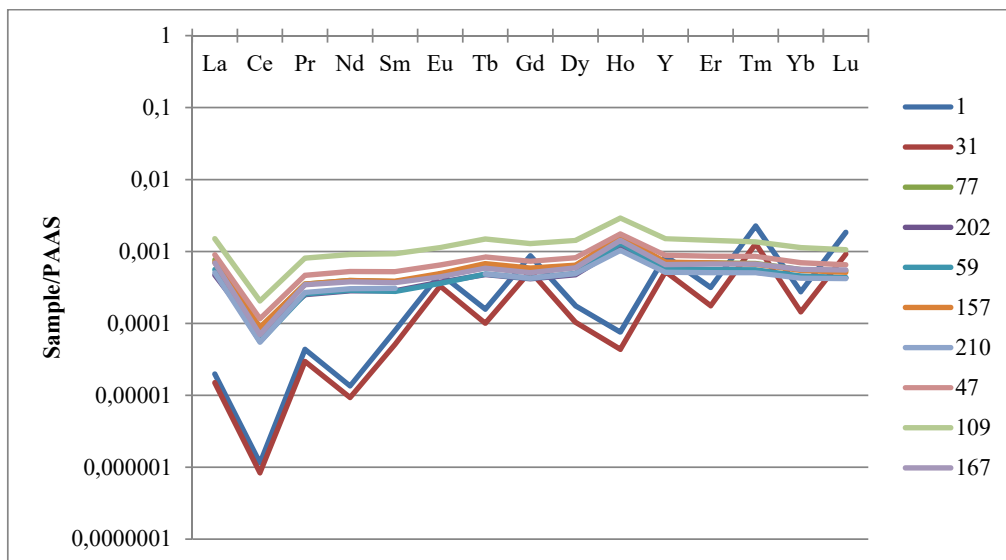


Figure 7. REE + Y element diagram of the stone samples from Hattusha, normalized to Post-Archaeon Australian Shale (PAAS) (Taylor and McLennan, 1985).

area surrounding Hattusha. Therefore, it can be stated that limestones with mainly Jurassic in age and with at least 1 m bed thickness cropping out around the region can be possible target for the provenance. Some samples indicate Cretaceous Sr isotope range values; this might be related to presence of Cretaceous aged blocks or error related to bulk rock analysis. However, majority of the samples and relationship of all other analysis support the main age interval is Jurassic. Presence of difference in microfacies of limestones and different geochemical properties indicate that Hittite builders probably used different limestone

quarries in different locations for setting up the building of the Great Temple.

Resistivity of building materials and their relationship with petrographic properties will be handled for a future study.

6. Conclusions

The limestone samples investigated were taken from different worked stone blocks of the wall socles of the Great Temple in Hattusha, Çorum (N-Turkey). This study combines the geochemical characteristics of the samples

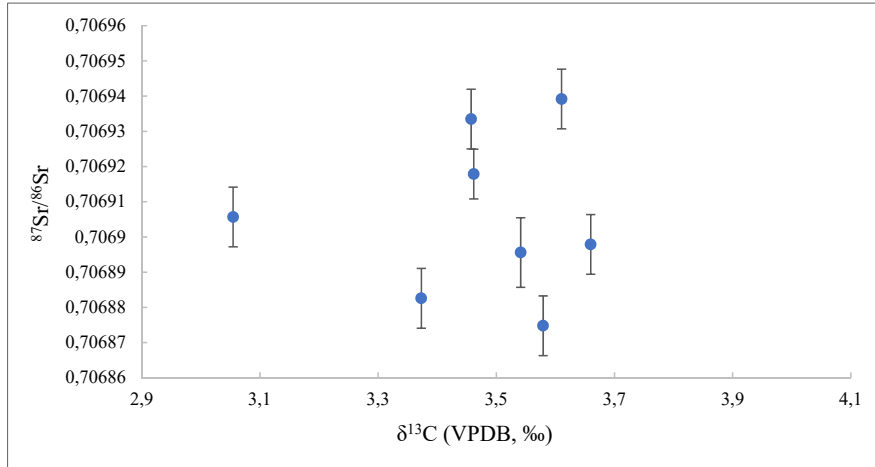


Figure 8. $^{87}\text{Sr}/^{86}\text{Sr}$ versus $\delta^{13}\text{C}$ plots of the stone samples from Hattusha.

with their petrographic identifications. We applied various geochemical methods including Sr isotope, stable isotope (C and O) and trace element geochemistry. The results show that the samples cluster in 5 different groups according to the stable isotope analyses and into two groups according to the trace element analyses. Trace element analyses reveal that the samples originated from seawater, which is deduced from the positive La, negative Ce, and elevated Y/Ho ratios. Sr isotope values indicate that the samples reveal Jurassic carbonates, although some show Cretaceous values (Rud'ko et al 2014).

From an archaeological point of view, the insight that the building was erected by using stones from probably five different sources is of great importance in understanding the process of its construction as well as of the acquisition of the building materials. The random distribution of the stones of the various groups does not indicate any obvious

clustering, although stones of group 2 seem to be in a slight quantitative majority. Accordingly, one may conclude that the characteristics of the individual groups of stones (such as hardness, etc.) did not influence the decision of the builders concerning where to use a given stone in a wall. Instead, criteria such as availability or, possibly, size might have been decisive.

Acknowledgments

We are thankful for the great supports of the Ministry of Culture and Tourism of Republic of Turkey, the German Archaeological Institute (Deutsches Archäologisches Institut, DAI), Department of Geological Engineering, Middle East Technical University, Ankara (Turkey) and Commonwealth Scientific and Industrial Research Organization, Brisbane (Australia). We also thank Duygu Tüfekçi Enginar for her help during field studies.

References

- Akcar N, Ivy-Ochs S, Alfimov V, Yilmaz IO, Schachner A et al. (2009). First results on determination of cosmogenic ^{36}Cl in limestone from the Yenice Kale Complex in the Hittite capital of Hattusha (Turkey). *Quaternary Geochronology* 4: 533–540.
- Akcar N, Alfimov V, Ivy-Ochs S, Yavuz V, Yilmaz IO et al. (2014). Origin of building stones in Yenice Kale Complex: Application of cosmogenic ^{36}Cl to archaeological problems. In: *Boğazköy-Hattuşa Ergebnisse der Ausgrabungen 24, Ausgrabungen und Forschungen in der westlichen Oberstadt von Hattusa I*. Schachner A, Seeher J (editors). de Gruyter, Berlin, 69–87.
- Braekmans D, Degryse P, Neyt B, Waelkens M, Poblome J (2016). Reconstructing regional trajectories: the provenance and distribution of Archaic to Hellenistic ceramics in Central Pisidia (South-West Turkey). *Archaeometry* 59: 472–492.
- Doğan-Alparslan M, Alparslan M (eds.) (2013). *Hititler – Hittites. Bir Anadolu İmparatorluğu – An Anatolian Empire*. Yapı Kredi Yayınları, İstanbul.
- Eggins SM, Woodhead JD, Kinsley LPJ, Mortimer GE, Sylvester P et al. (1997). A simple method for the precise determination of P40 trace elements in geological samples by ICPMS using enriched isotope internal standardisation. *Chemical Geology* 134: 311–326.
- Flügel E (2010). *Microfacies of carbonate rocks: analysis, interpretation and application*. Springer, Berlin.
- Hunt AMW (2013). Development of quartz cathodoluminescence for the geological grouping of archaeological ceramics: firing effects and data analysis. *Journal of Archaeological Sciences* 40: 2902–2912.

- Kamber BS, Greig A, Schoenberg R, Collerson KD (2003). A refined solution to Earth's hidden niobium: implications for evolution of continental crust and mode of core formation. *Precambrian Research* 126: 289–308.
- Kazancı N, Suludere Y, Mülazımoğlu NS, Tuzcu S, Mengi H et al. (2008). Milli parklarda jeolojik miras – 4, Boğazköy–Alacahöyük tarihi milli parkı (Çorum). *Doğa koruma ve milli parklar genel müdürlüğü jeolojik mirası koruma derneği* (in Turkish).
- Price TD, Burton JH (2012). *An introduction to archaeological chemistry*. Springer, New York, USA.
- Rud'ko SV, Kuznetsov AB, Piskunov VK (2014). Sr Isotope Chemostratigraphy of Upper Jurassic Carbonate Rocks in the Demerdzhi Plateau (Crimean Mountains). *Stratigraphy and Geological Correlation* 22 (5): 494–506.
- Schachner A (2011). Hattuscha. Auf den Spuren des sagenhaften Großreichs der Hethiter, Beck Verlag, München (in German).
- Schachner A (2019). Hattuša. Efsanevi Hitit İmparatorluğu'nun izinde, Homer Yayınları, İstanbul, Turkey.
- Schachner A (2020). The Great Temple at Hattuša. Some preliminary interpretations. In: *Cult, temple, sacred spaces. Cult practices and cult spaces in Hittite Anatolia and neighbouring cultures*. Steitler CH and Görke S (editors). *Studien zu den Boğazköy-Texten* 66. Wiesbaden: Harrasowitz.
- Schachner A. Building for King and Country: Architecture as a Symbol of the Hittite Empire, in: St. de Martino, *The Hittites*, de Gruyter, Berlin (in press).
- Siegesmund S, Török A (2014). Building stones, In: *Stone in Architecture*. Siegesmund S and Snethlage R (editors), Springer, Berlin, Heidelberg, Germany, 11–95.
- Şenel M, Aydal N, Papak İ, Coşkun A, Kapucu M et al. (2002). 1/500 000 scale Geological map of Turkey, Geological Research Department of the General Directorate of Mineral Research and Exploration. MTA, Ankara, Turkey.
- Taylor SR, McLennan SM (1985). *The Continental crust: Its composition and evolution*. Blackwell, Oxford.
- Yılmaz IO, Altiner D, Schachner A (2014). Sedimentological and paleontological approach for the provenance of the wall blocks of Hittites in the Yenicekale Hill, Bogazkoy, Turkey. In: *Boğazköy-Hattuša, Ergebnisse der Ausgrabungen 24, Ausgrabungen und Forschungen in der westlichen Oberstadt von Hattusa*. I. Schachner A and Seeher J (editors), de Gruyter GmbH, Berlin, 62–68.